Monel Contribution to AC Losses in MgB_2 Wires in Frequencies Up To 18 kHz

Yasha Nikulshin, Shuki Wolfus, Alex Friedman, Vladmir Ginodman, Gianni Grasso, Matteo Tropeano, Gianmarco Bovone, Maurizio Vignolo, Carlo Ferdeghini, and Yosef Yeshurun

***Abstract*—AC losses for a wide range of ac amplitudes and frequencies have been studied in magnesium diboride (MgB_2) superconducting wire with 36 filaments and Monel sheath at different temperatures and dc current levels. The results show a strong nonlinear frequency dependence below 1 kHz, which crosses over to a more moderate linear behavior at frequencies up to 18 kHz. Surprisingly, the introduction of dc current causes a significant reduction in the ac losses. Finite element simulations yield ac losses consistent with that observed experimentally. The simulations show that the magnetic Monel sheath is a dominant source for ac losses in zero dc current and that nonzero dc current saturates the magnetization, thus reducing the ac losses.**

***Index Terms*—AC losses, finite element method (FEM), magnesium diboride (MgB_2), superconducting magnetic energy storage (SMES), superconducting filaments and wires.**

I. Introduction

SINCE its discovery in 2001 [1], magnesium diboride (MgB_2) has become one of the most attractive superconducting materials for applications. The relatively low cost of MgB_2 wires and its moderately high critical temperature of $\sim$39 K made it a promising candidate for use in power applications such as superconducting magnetic energy storage (SMES) [2]–[5] and high voltage direct current (HVDC) lines [6]–[8]. Although the base power frequency is 50/60 Hz, both applications utilize the pulsewidth modulation (PWM) technique [9] with frequencies of several kilohertz for conversion from dc current to ac current. In such applications, the superconductor carries dc current on which ac current ripples are superimposed due to the very nature of high frequency switching used in the PWM technique with a wide-range duty cycle. In SMES, ac ripples are present both in the standby mode, where switching is used only for compensating the current decay, and in charge and discharge cycles, where the power is converted from ac to dc or vice versa. A typical PWM base frequency is 3 kHz and the ripples are usually nonsinusoidal. It is, thus, important to characterize the frequency dependence of the losses up to, say, the fifth harmonics (i.e., 15 kHz). Therefore, it is important to measure the ac losses in this frequency range and understand its origin. Extensive research work has been done on ac losses in MgB_2 wires, tapes, and cables [10]–[26]. In several papers, e.g., [11], [14]–[16], the main goal was the investigation of the magnetization ac losses in MgB_2 wires in the presence of external magnetic field but without transport current. Many others focused on transport ac losses [17], [18], [23]–[26] but without dc current. Several others [19]–[21] reported on the losses for the combination of dc current and ac ripples but at frequencies much lower than required for typical PWM use. Thus, the available research works cover only partially the conditions required for SMES/HVDC applications. The need to explore the behavior of MgB_2 superconducting wires at high frequencies is evident and turns crucial as the potential for high-power MgB_2 applications becomes realistic.

For practical applications, the study of ac losses is of extreme importance especially for conduction-cooled superconductors where cooling power is very limited. In such cooling, failure to estimate the energy dissipated within the coil under real operating conditions may result in insufficient cooling power to maintain a constant operating temperature and eventually a thermal runaway in the superconductor. We measured the ac losses in the MgB_2 wire produced by Columbus Superconductors [27] with 36 filaments and Monel outer sheath, using an electrical method [28]. For this purpose, a unique experimental setup, based on conduction cooling and electrically nonconducting cooling bus, designed for measuring ac loss in superconducting wires and coils in a frequency range up to 18 kHz was built. To clearly understand the loss mechanisms, a two-dimensional (2-D) finite element method (FEM) simulation [29], [30] based on H-formulation, was adopted. The numerical model calculated the spatial and temporal dependence of the magnetic field, taking as input the electrical properties of the superconductor described by the *E–J* power law and the electrical resistivity and nonlinear magnetic properties of the Monel.

Manuscript received April 19, 2017; revised February 26, 2018; accepted May 17, 2018. Date of publication May 31, 2018; date of current version July 17, 2018. The design and development of the experimental setup was supported by the Israel Ministry of National Infrastructures, Energy, and Water. The measurements of the Columbus wires have been performed in the framework of the Israeli-Italian Scientific and Technological Cooperation program supported by the Israel Ministry of Science Technology and Space, and the Italian Ministry of Foreign Affairs. The work of Y. Nikulshin was supported by a Ph.D. grant from the Ministry of Science Technology and Space, Israel. This paper was recommended by Associate Editor N. Amemiya. *(Corresponding author: Yasha Nikulshin.)*

Y. Nikulshin, S. Wolfus, A. Friedman, V. Ginodman, and Y. Yeshurun are with the Institute of Superconductivity, Department of Physics, Bar-Ilan University, Ramat-Gan 5290002, Israel (e-mail: yasha.nick@gmail.com).

G. Grasso and M. Tropeano are with Columbus Superconductors, Genova 16133, Italy.

G. Bovone, M. Vignolo, and C. Ferdeghini are with the CNR Institute SPIN, Genova 16152, Italy.

Color versions of one or more of the figures in this paper are available online at http://ieeexplore.ieee.org.

Digital Object Identifier 10.1109/TASC.2018.2841926

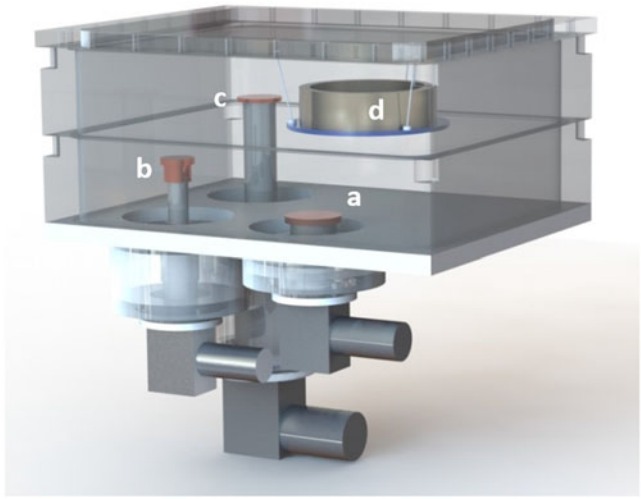

Fig. 1. Schematic description of the cryostat assembly. (a) Edwards 0/40. (b) Edwards 6/30. (c) Sumitomo RDK-408D2. (d) Superconducting sample (coil in this scheme).

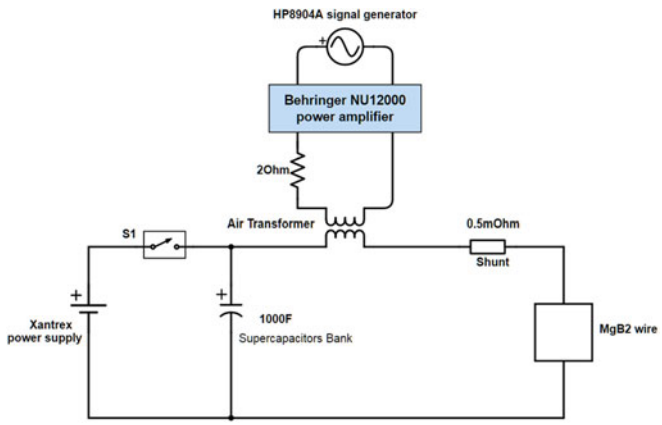

Fig. 2. Electrical scheme of the measurement system.

II. Experimental

All the results depicted in this paper were acquired in a home-made system designed for measurements of ac losses in superconducting wires, tapes, and coils. The cryogenic part of the system, described schematically in Fig. 1, comprises a cryostat and three cryocoolers. The cryostat is made of Delrin to eliminate eddy currents in the cryostat walls due to alternating magnetic fields, and its volume is sufficient to contain coils of diameters up to 60 cm. The cryocoolers—Edwards 0/40, Edwards 6/30, and Sumitomo RDK-408D2—are capable of reaching base temperatures of 50, 25, and 3.8 K, respectively. The Edwards 0/40 and the first cooling stage of the 6/30 are used for cooling the current leads and peripheral cabling, while the Sumitomo cold-head cools the sample. YBCO current leads to connect the 25 and 4 K stages.

AC loss measurements are based on the electrical method [28], namely, measuring the time integral of the product $I{\cdot}V$ waveforms per cycle. Electrical scheme of the measurement setup is presented in Fig. 2.

DC current is supplied by Xantrex (20–300) power supply connected in parallel to a 1000 F supercapacitor bank. The capacitor bank serves as a high-pass filter to eliminate ac currents passing through the dc power supply and filter high-frequency noise from the switching dc power supply. AC current is driven by a Behringer NU12000 6 kW/ch high-power audio amplifier and coupled to the measurement circuit through an air transformer connected in series to the main loop. The system, thus, allows superimposing dc and ac currents through the measured sample. Voltage taps are mounted on the sample, 50 mm apart. The total length of the wire is 180 mm. The current through the wire and the voltage across the taps are measured by the Newtons4th PPA5510 high-precision power analyzer. The instrumentation is connected and controlled by MATLAB environment with feedback loop to stabilize the currents.

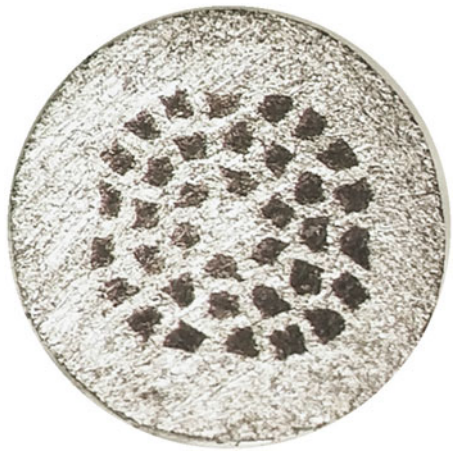

Fig. 3. Image of the cross-section of a 1.3 mm diameter, 36 filamentary MgB_2 wire with a Monel outer sheath.

The measurements described here were conducted on a 1.3 mm diameter, 36 filamentary round MgB_2 wire with the Monel matrix, produced by Columbus Superconductors. The critical current of a similar wire is about 1000 A at 10 K in self-field [22]. The filaments are distributed in three layers, as shown in Fig. 3. The MgB_2 wire sample is cast in alumina grains of various sizes impregnated with epoxy to ensure thermal conductivity and efficient heat removal while making sure that there are no electrically conductive materials in the range of at least 15 mm from the sample.

In realistic use of superconductors in power applications, the dc current is in the range of hundreds or even thousands of Amperes, while ac current components are only a few % of it at most. The losses were measured with amplitudes of ac current from 0.5 to 8 A_{rms}, which represent the relatively small fraction of high dc current amplitude. However, our experimental setup (see Fig. 2) does not allow for currents above ~50 A due to the small air transformer, which limited the dc current to be only 40 A. Despite this relatively small dc amplitude, the measurements results show virtually no influence of further increase of dc current.

III. Results

Sinusoidal ac currents of amplitudes from 0.5 to 8 A_{rms} and frequencies from 57 Hz to 18 kHz were driven through the sample, superimposed on dc currents from zero to 40 A in

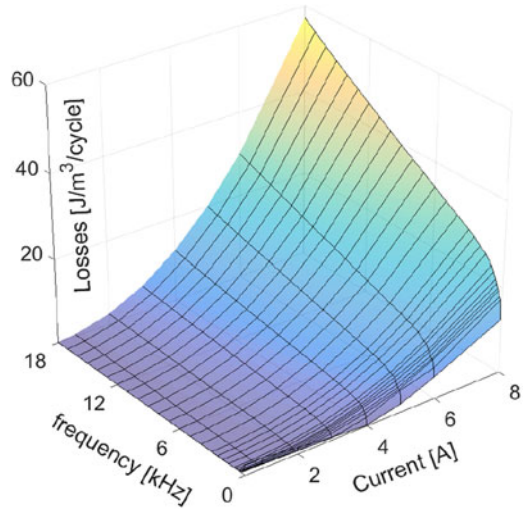

Fig. 4. Energy losses as a function of ac current and frequency.

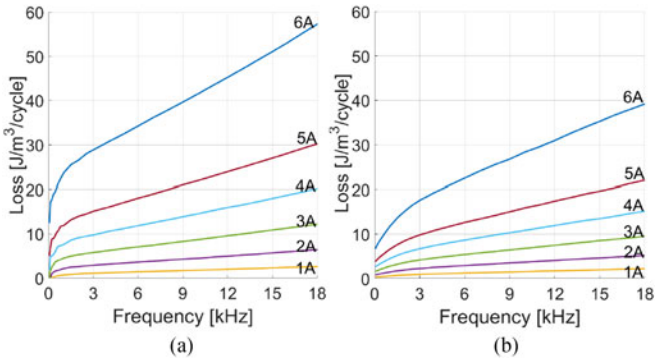

Fig. 5. AC losses as a function of frequency for the indicated ac current amplitude for (a) $I_{\rm dc} = 0$ and (b) $I_{\rm dc} = 40$ A.

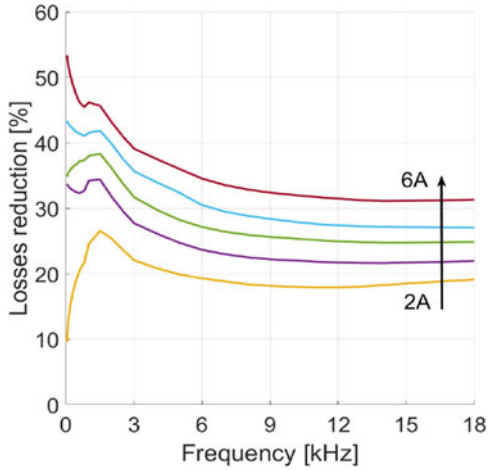

Fig. 6. Loss reduction [%] due to the dc current of 40 A for ac currents amplitudes of 2, 3, 4, 5, 6 A.

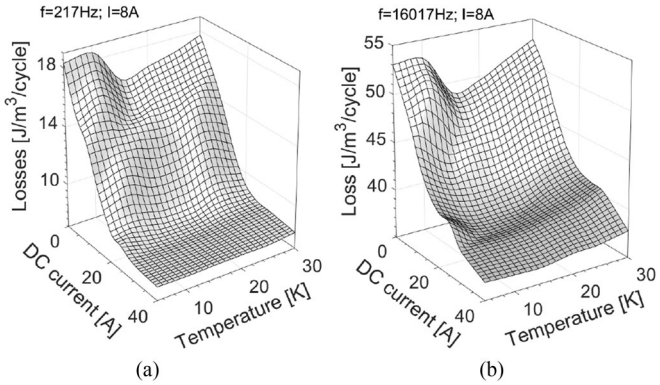

Fig. 7. AC losses as a function of dc current bias and temperature for (a) 217 Hz, 8 A ac current and (b) 16 017 Hz, 8 A ac current.

self-field. The measurements were performed in a temperature range from 5.5 to 35 K. Fig. 4 shows the measured energy loss per wire volume per cycle at 10 K as a function of the ac current amplitude and frequency, in zero dc current. As expected, the energy loss increases upon increasing either amplitude or frequency. As depicted in Fig. 5(a), we observe a strong nonlinear dependence of the loss on the frequency. Up to $\sim$1 kHz there is a fast increase of the ac losses with frequency, crossing over to a slow, approximately linear increase at high frequencies. This change in the behavior suggests a crossover between two dominant mechanisms of ac loss formation. These mechanisms will be discussed in the next section.

Fig. 5(b) shows the frequency dependence of the loss with a dc bias current of 40 A. Comparing Fig. 5(a) and (b), it is apparent that the dc current reduces the loss significantly, namely, losses in the presence of a dc bias current are much less than those without dc bias. In Fig. 6, we present this loss reduction resulting from the additional dc current and show that losses in the 40 A dc bias case are reduced by $\sim$50% in comparison with the zero dc bias case. As discussed later, this surprising behavior is attributed to the magnetic properties of the Monel matrix.

Clearly, the ac losses depend on the ac current amplitude. The higher the ac amplitude, the larger the relative loss reduction (see Fig. 6). We emphasize again that we observe different behaviors for lower and higher frequencies ranges. This can play a significant role in designing devices for power application where not only grid frequencies (50/60 Hz) but also much higher frequencies exist, like in the case of SMES or switching modulations as PWM.

To have a clearer picture of the ac losses in the sample, Fig. 7(a) and (b) presents the ac losses as a function of the dc current and temperature for $I_{\rm ac} = 8$ A and two representing frequencies: 217 and 16 017 Hz. Apparently, at low frequencies [see Fig. 7(a)], the initial increase of dc current results in a gradual decrease in the ac losses, reaching a plateau around $\sim$20 A. A different behavior is observed at high frequencies [see Fig. 7(b)], where such a plateau is not reached and the decrease in ac losses is more moderate at high dc currents. The temperature dependence is also nontrivial. In both cases, we observe higher losses for temperatures below 10 K, with a minimum at 15 K. The losses then gradually increase with the temperature from 15 to 35 K. Since dc current levels are way below the critical current, such a strong temperature dependence is not expected.

Eddy currents loss per cycle increase linearly with frequency, but the hysteresis loss in superconducting filaments is expected

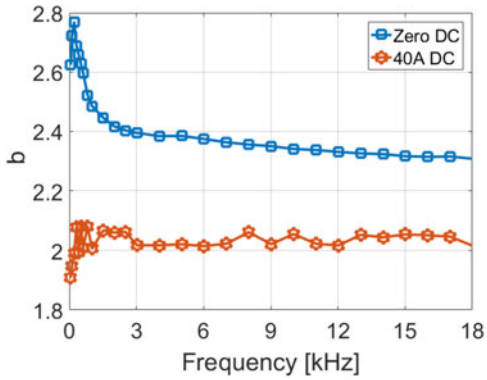

Fig. 8. Exponent *b* of power law-fit of the current amplitude versus frequency for zero dc bias (squares) and 40 A dc bias (stars).

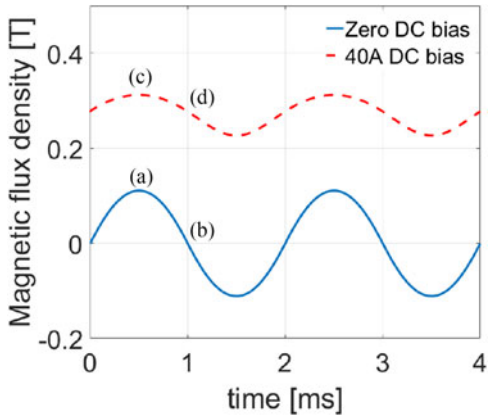

Fig. 9. Time dependence of the magnetic flux density in the outer part of the wire, for (a) zero dc, max ac current, (b) zero dc, zero ac, (c) 40 A dc, max ac, and (d) 40 A dc, zero ac.

to be frequency independent [31]. Additional step of data analysis is, therefore, a power-law fit of the loss Q, $Q(I) \sim I^b$, for every frequency of the ac current both for zero and for 40 A dc current. Fig. 8 shows the frequency dependence of the exponent b derived from the fit versus frequency. For zero dc bias, the exponent value is close to 3 at low frequencies, indicating magnetic hysteresis loss in the MgB_2 superconducting filaments. As frequency increases, the exponent decreases, indicating that eddy currents and magnetic hysteresis losses in the Monel matrix become dominant. We suggest that the eddy current losses in the Monel are dominant at the frequency range discussed here because of its low electrical resistivity and high permeability. A similar conclusion, though for different materials and different frequency ranges, was suggested also in [10] and [12].

As is clear from Fig. 8, the exponent b in the presence of 40 A dc bias current is practically frequency independent and close to 2. This value is quite counterintuitive since magnetic saturation of the Monel should reduce the magnitude of eddy currents and virtually eliminate the hysteresis loss in the Monel, leaving the MgB_2 hysteresis dominant with exponent b of $\sim$3 (at least at low frequencies). Further investigations of the magnetic fields distributions and currents in the wire are necessary to explain this behavior.

IV. Simulations

To better understand the origin of the reduction in the ac losses, we used an FEM in COMSOL software package to analyze a model of the wire based on similar properties and conditions as in the experimental section. A time-dependent H-formulation 2-D model was used. A 2-D space implies infinite wire length. The total current in the wire is relatively small and flows only in 18 filaments out of 36 on the outer layer of the wire. The whole inner part of the wire is screened from the magnetic field. Due to the symmetry, only azimuthal magnetic field is present, which does not cross any area between the filaments and thus does not produce any filament coupling effect. This allows us to save computational time by simulating only 1/18 of the wire. The total current in the wire was taken as $I_{\rm ac}\sin(2\pi ft) + I_{\rm dc}(1 - e^{-5ft})$, where $I_{\rm ac}$ and $I_{\rm dc}$ are ac and dc current amplitudes, respectively, and f is the frequency. The exponential term that multiplies $I_{\rm dc}$ is required since the time-dependent H-formulation model has to start from zero field. The dc current was either zero or 40 A. In both cases, the ac current was 8 $A_{\rm rms}$ at 500 Hz. The simulation ran for 15 cycles to eliminate the initial current ramping effects. The losses were calculated only for the last cycle by surface integration of the $J{\cdot}E$ term over all the filaments and the Monel independently. The Monel material was described by the μ–H curve with saturation at 0.2 T (a value obtained in independent measurements exploiting a "quantum design" MPMS magnetometer at low temperatures and fitting the data to $\mu_r = 1 + c_1(1 - e^{-H/c_2})/H)$ with $C_1 = 155\,600$ and $C_2 = 905$). The Monel electrical resistivity is $3.65{\cdot}10^{-7}$ $\Omega{\cdot}$m [2].

Due to the nonlinearity of the magnetization of the Monel, the magnetic field at a specific point depends on its distance from the filament. This led us to average the magnetic field over the Monel area outside the filament. Fig. 9 displays the spatial average of the magnetic flux density versus time in the outer part of the wire for both cases during two cycles. The difference in the flux density between maximum ac current (a) and zero ac current (b) with no dc current is 0.11 T, while in the case of 40 A dc current (c and d), the difference is only 0.04 T.

Fig. 10 shows four snapshots of the solution for the same points (a, b, c, d). The red-blue color code represents the current density inside the superconducting filaments and the blue-white code stands for the magnetic flux density in the Monel sheath. For the convenience of the presentation, only 3 of the 18 outer filaments are shown. In all cases, the current density is concentrated on the outer part of the filaments and only small portion of the filament's cross-section carries the current. The central part of the wire is totally screened of currents and magnetic fields. Electric field is induced in the metal sheath, and thus eddy currents losses are proportional to the magnetic-field time derivative (dB/dt). When no dc bias current flows in the wire, the ac current causes a maximum magnetic flux density change during the cycle due to high permeability of the Monel at low magnetic fields. On the contrary, introducing a 40 A dc current saturates the Monel sheath and reduces the permeability, thus

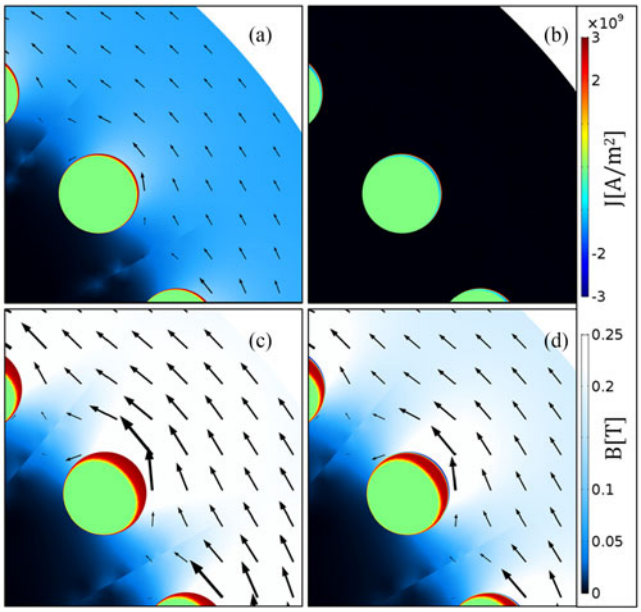

Fig. 10. Snapshot of simulation results. RGB color code stands for current density in the MgB_2 filaments, brightness of blue stands for magnetic flux density in the Monel. The panels describe *J* and *B* for the four cases marked in Fig. 8, namely, (a) zero dc, max ac current, (b) zero dc, zero ac, (c) 40 A dc, max ac, and (d) 40 A dc, zero ac. The thin blue area in (d) at the edge of the filament corresponds to the decrease of the total current compared to (c).

reducing the magnetic flux change and the eddy current losses, consistent with the experimental results.

At selected amplitudes and frequency, we see total domination of losses in the Monel ($1.08 \cdot 10^{-7}$ J/cycle) over losses inside MgB_2 filaments ($2.04 \cdot 10^{-8}$ J/cycle). However, we see only about 50% loss reduction in the experiment and much higher reduction in permeability when the Monel is saturated (at least ten times). The cause of this difference might be the fact that we use the dc permeability of the Monel in the model. Ferromagnetic materials behave differently when ac magnetic fields are present especially at low temperatures. As was shown in [3], the Monel used in MgB_2 wires has its own hysteresis losses. In fact, a frequency-dependent hysteresis mechanism in the Monel is involved, reducing the effective ac permeability of the material and introducing additional losses [4].

V. Summary and Conclusion

We presented the first results of ac loss measurements of MgB_2 wires for frequencies up to 18 kHz, exploiting a recently built novel system that enables a superposition of dc and ac currents in the sample while eliminating the electromagnetic interference of the cryostat. The measurements and the accompanying simulations have shown a significant loss reduction due to dc current. This effect originates from the magnetic saturation of the Monel sheath by high dc current that results in a pronounced reduction in the eddy currents.

For validation of the experimental result, a finite element model has been built. The simulation clearly shows the saturation of the Monel in the outer area of the wire, resulting in a reduction in the magnetic flux change during the ac cycle, and hence a reduction in the eddy currents.

Based on our experimental results and simulations, we conclude that under operating conditions typical of SMES, it is important to minimize the use of the magnetic matrix and search for alternatives to the Monel. Resistive and nonmagnetic matrix is preferable for applications utilizing high frequency switching. If the Monel is still used, it is crucial to magnetically saturate the matrix in all parts of the wire.

Acknowledgment

The authors thank M. Ainslie for help with the finite element method modeling.

References

[1] J. Nagamatsu, N. Nakagawa, T. Muranaka, Y. Zenitani, and J. Akimitsu, "Superconductivity at 39 K in magnesium diboride," *Nature*, vol. 410, no. 6824, pp. 63–64, Mar. 2001.

[2] A. Friedman, N. Shaked, E. Perel, M. Sinvani, Y. Wolfus, and Y. Yeshurun, "Superconducting magnetic energy storage device operating at liquid nitrogen temperatures," *Cryogenics*, vol. 39, no. 1, pp. 53–58, Jan. 1999.

[3] M. H. Ali, S. Member, B. Wu, and R. A. Dougal, "An overview of SMES applications in power and energy systems," *IEEE Trans. Sustain. Energy*, vol. 1, no. 1, pp. 38–47, Apr. 2010.

[4] Y. Oga, S. Member, S. Noguchi, and M. Tsuda, "Comparison of optimal configuration of SMES magnet wound with MgB_2 and YBCO conductors," *IEEE Trans. Appl. Supercond.*, vol. 23, no. 3, Jun. 2013, Art. no. 5700204.

[5] A. M. Wolsky, "The status and prospects for flywheels and SMES that incorporate HTS," *Phys. C, Supercond.*, vols. 372–376, no. 3, pp. 1495–1499, Aug. 2002.

[6] V. V. Kostyuk *et al.*, "Experimental hybrid power transmission line with liquid hydrogen and MgB_2-based superconducting cable," *Tech. Phys. Lett.*, vol. 38, no. 3, pp. 279–282, Mar. 2012.

[7] A. Ballarino *et al.*, "The BEST PATHS project on MgB_2 superconducting cables for very high power transmission," *IEEE Trans. Appl. Supercond.*, vol. 26, no. 3, Apr. 2016, Art. no. 5401705.

[8] R. Rudervall, J. Chapentier, and R. Sharma, "High voltage direct current (HVDC) transmission systems technology review paper," in *Proc. Energy Week*, 2000, pp. 1–19.

[9] D. G. Holmes and T. A. Lipo, *Pulse Width Modulation for Power Converters: Principles and Practice*. Hoboken, NJ, USA: Wiley, 2003.

[10] M. Majoros, M. D. Sumption, M. A. Susner, M. Tomsic, M. Rindfleisch, and E. W. Collings, "AC losses in MgB_2 multifilamentary strands with magnetic and non-magnetic sheath materials," *IEEE Trans. Appl. Supercond.*, vol. 19, no. 3, pp. 3106–3109, Jun. 2009.

[11] J. Kováč, J. Šouc, P. Kováč, and I. Hušek, "Magnetization ac losses in MgB_2 wires made by IMD process," *Supercond. Sci. Technol.*, vol. 28, 2015, Art. no. 015013.

[12] J. Kováč, J. Šouc, P. Kováč, and I. Hušek, "AC losses of single-core MgB_2 wires with different metallic sheaths," *Phys. C, Supercond. Appl.*, vol. 519, pp. 95–99, Dec. 2015.

[13] K. Kajikawa, R. Osaka, T. Nakamura, M. Sugano, and T. Wakuda, "AC loss evaluation of MgB_2 superconducting windings located in a stator core slot with a finite-element method," *J. Supercond. Nov. Magn.*, vol. 24, nos. 1–2, pp. 987–991, Sep. 2010.

[14] C. Zhou *et al.*, "Intra-wire resistance and ac loss in multi-filamentary MgB_2 wires," *Supercond. Sci. Technol.*, vol. 26, no. 2, 2013, Art. no. 25002.

[15] S. Safran, J. Šouc, F. Gömöry, P. Kovac, and A. Gencer, "Experimentally determined magnetization ac losses of mono and multifilamentary MgB_2 wires," *J. Supercond. Nov. Magn.*, vol. 26, no. 5, pp. 1557–1561, Dec. 2012.

[16] S. Choi *et al.*, "Magnetization loss of MgB_2 superconducting wire at various temperatures," *J. Supercond. Nov. Magn.*, vol. 26, pp. 1531–1535, 2013.

[17] K. Kajikawa *et al.*, "AC losses in monofilamentary MgB_2 round wire carrying alternating transport currents," *Supercond. Sci. Technol.*, vol. 23, no. 4, Apr. 2010, Art. no. 45026.

[18] F. Wan, M. D. Sumption, M. A. Rindfleisch, M. J. Tomsic, and E. W. Collings, "Architecture and transport properties of multifilamentary MgB_2 strands for MRI and low ac loss applications," *IEEE Trans. Appl. Supercond.*, vol. 27, no. 4, Jun. 2017, Art. no. 6200105.

[19] C.-E. Bruzek *et al.*, "Cable conductor design for the high-power MgB_2 dc superconducting cable project within BEST PATHS," *IEEE Trans. Appl. Supercond.*, vol. 27, no. 4, Jun. 2017, Art. no. 4801405.
[20] V. Lahtinen, E. Pardo, J. Šouc, M. Solovyov, and A. Stenvall, "Ripple field losses in direct current biased superconductors: Simulations and comparison with measurements," *J. Appl. Phys.*, vol. 115, no. 11, Mar. 2014, Art. no. 113907.
[21] D. Liu, H. Polinder, N. Magnusson, J. Schellevis, and A. B. Abrahamsen, "Ripple field ac losses in 10-MW wind turbine generators with a MgB_2 superconducting field winding," *IEEE Trans. Appl. Supercond.*, vol. 26, no. 3, Apr. 2016, Art. no. 5204205.
[22] G. Escamez *et al.*, "Experimental characterization of the constitutive materials of MgB_2 multi-filamentary wires for the development of 3D numerical models," *Supercond. Sci. Technol.*, vol. 30, no. 3, Mar. 2017, Art. no. 34008.
[23] A. Kundu *et al.*, "Magnesium-diboride-based prototype ELM coil fabrication, dc characterization, and ac transport-current-induced loss estimation: A feasibility study," *IEEE Trans. Appl. Supercond.*, vol. 25, no. 4, Aug. 2015, Art. no. 4701307.
[24] S. Choi *et al.*, "Prediction of ac losses in MgB_2 superconducting wires as a function of transport currents and temperatures," *IEEE Trans. Appl. Supercond.*, vol. 22, no. 3, Jun. 2012, Art. no. 6200404.
[25] A. Malagoli, C. Bernini, V. Braccini, C. Fanciulli, G. Romano, and M. Vignolo, "Fabrication and superconducting properties of multifilamentary MgB_2 conductors for ac purposes: Twisted tapes and wires with very thin filaments," *Supercond. Sci. Technol.*, vol. 22, no. 10, Oct. 2009, Art. no. 105017.
[26] E. Young, M. Bianchetti, G. Grasso, and Y. Yang, "Characteristics of ac loss in multifilamentary MgB_2 tapes," *IEEE Trans. Appl. Supercond.*, vol. 17, no. 2, pp. 2945–2948, Jun. 2007.
[27] Columbus Superconductors SPA. [Online]. Available: http://columbus superconductors.com/
[28] J. J. Rabbers, B. Ten Haken, and H. H. J. Ten Kate, "Advanced ac loss measurement methods for high-temperature superconducting tapes," *Rev. Sci. Instrum.*, vol. 72, no. 5, pp. 2365–2373, 2001.
[29] M. D. Ainslie, T. J. Flack, and A. M. Campbell, "Calculating transport ac losses in stacks of high temperature superconductor coated conductors with magnetic substrates using FEM," *Phys. C, Supercond. Appl.*, vol. 472, no. 1, pp. 50–56, 2012.
[30] M. D. Ainslie, "Transport ac loss in high temperature superconducting coils," Doctoral dissertation, Univ. Cambridge, Cambridge, U.K., 2012.
[31] W. T. Norris, "Calculation of hysteresis losses in hard superconductors carrying ac: Isolated conductors and edges of thin sheets," *J. Phys. D, Appl. Phys.*, vol. 3, no. 4, Apr. 1970, Art. no. 308.
[32] J. Ekin, *Experimental Techniques for Low-Temperature Measurements*. London, U.K.: Oxford Univ. Press, 2006.
[33] G. Bertotti, *Hysteresis in Magnetism: For Physicists, Materials Scientists, and Engineers*. New York, NY, USA: Academic, 1998.

Authors' biographies not available at the time of publication.